

## Theoretical investigation of a Mn-doped Si/Ge heterostructure

J. T. Arantes,<sup>1</sup> Antônio J. R. da Silva,<sup>1</sup> and A. Fazzio<sup>1,2</sup>

<sup>1</sup>Instituto de Física, Universidade de São Paulo, Caixa Postale 66318, 05315-970 São Paulo, São Paulo, Brazil

<sup>2</sup>Centro Internacional de Física da Matéria Condensada, Universidade de Brasília, Caixa Postale 04513, 70904-970 Brasília, Distrito Federal, Brazil

A. Antonelli

Instituto de Física “Gleb Wataghin,” Universidade Estadual de Campinas, Caixa Postale 6165, 13083-970 Campinas, São Paulo, Brazil

(Received 1 September 2006; revised manuscript received 29 November 2006; published 9 February 2007)

We investigate, through *ab initio* density-functional theory calculations, the electronic and structural properties of neutral Mn impurities at tetrahedral interstitial and substitutional sites in both Si and Ge layers of a Si/Ge heterostructure. We conclude that substitutional Mn at the Ge layers is more stable than interstitial Mn at the Si layers by approximately 0.45 eV, and we estimate an energy barrier of at least 1.12 eV to diffuse away from these most stable substitutional sites. Mn has a magnetic moment in the heterostructure that is similar to that in the bulk, and for the compressed Ge layer the Mn-Mn exchange interaction is always weakly antiferromagnetic. Varying the lattice constant of the substrate, the Mn-Mn ground state becomes ferromagnetic. This result opens up the possibility of manipulating the interaction between Mn impurities at Ge layers grown over a Si<sub>1-x</sub>Ge<sub>x</sub> substrate by changing  $x$ .

DOI: 10.1103/PhysRevB.75.075316

PACS number(s): 75.30.Hx, 75.50.Pp, 75.70.Cn, 75.75.+a

### I. INTRODUCTION

Diluted magnetic semiconductors (DMSs) have spurred an intense research activity in the past few years, motivated largely by the possibilities of control and integration of both spin and charge degrees of freedom in useful devices.<sup>1</sup> To this end, it is no surprise that this large body of research is further motivated by the fact that III-V semiconductors, and (Ga,Mn)As in particular, present a ferromagnetic behavior at appropriate Mn doping and temperature.<sup>1</sup> However, there is no doubt that from a technological point of view, there would be a great interest in having type-IV DMS ferromagnetic materials.<sup>2,3</sup> Reports of ferromagnetism in Mn<sub>x</sub>Ge<sub>1-x</sub> DMS (Ref. 4) have been recently made; however, no similar results have so far been reported for Si. Aside from the great difficulty of doping Si with transition metals due to the tendency to form silicides, there is an important difference between Mn doping in Si and Ge: in Si, a Mn impurity favors the interstitial site, whereas in Ge, it prefers the substitutional site.<sup>5</sup> As a consequence, a Mn substitutional impurity in Ge cannot diffuse as easily as an interstitial Mn in Si,<sup>6-8</sup> allowing the introduction of a large enough number of impurities without their diffusion and subsequent clustering.

Even though it may be almost impossible to grow a pure Si DMS material, it may still be possible to obtain a Mn:Si<sub>1-x</sub>Ge<sub>x</sub> alloy<sup>5</sup> with ferromagnetic properties similar to those of Mn<sub>x</sub>Ge<sub>1-x</sub> DMS. Therefore, it may be possible to envision Si/Ge heterostructures where ferromagnetic Mn<sub>x</sub>Ge<sub>1-x</sub> (or Mn:Si<sub>1-x</sub>Ge<sub>x</sub>) DMS layers may be used either to inject polarized electrons in the Si layers or as spin filters, all integrated with the current Si technology.

One important aspect that has to be considered before one even starts to take these ideas more seriously is the necessity for the Mn impurities in the Ge layers to be thermodynamically and kinetically stable against migration toward the Si layers. This means that the formation energy for a substitutional Mn in the Ge layers (Mn<sub>Ge</sub>) must be significantly

smaller than that for an interstitial impurity in the Si layers (Mn<sub>Si</sub>) and that the migration energy barrier for the Mn<sub>Ge</sub> should be sufficiently high as compared to the thermal energy. This is precisely the point we want to address in the present work. We investigate, using state-of-the-art *ab initio* calculations, the relative stability of neutral Mn impurities in tetrahedral interstitial and substitutional sites, in both Si and Ge atomic layers, for a model Si/Ge heterostructure. Our results allow us to conclude that (i) a Mn<sub>Ge</sub> is more stable than a Mn<sub>Si</sub> by approximately 0.45 eV and (ii) the energy migration barrier for diffusion of a Mn<sub>Ge</sub> is at least 1.12 eV, which indicates that once a ferromagnetic Mn<sub>x</sub>Ge<sub>1-x</sub> layer is grown on top of a Si substrate, it will be stable with respect to the transfer of Mn atoms to the Si interstitial sites.

### II. COMPUTATIONAL METHODS

All our results are obtained via total-energy *ab initio* calculations based on the spin-polarized density-functional theory within the generalized gradient approximation.<sup>9</sup> We have used ultrasoft pseudopotentials<sup>10</sup> and a plane-wave expansion up to 227.15 eV, as implemented in the VASP code.<sup>11</sup> For bulk calculations, we have used a 64 atom (Si or Ge) cubic supercell with a (3 × 3 × 3) Monkhorst-Pack Brillouin-zone sampling. For the Si/Ge heterostructure, we have used a fcc-based supercell containing 192 sites distributed in 12 atomic layers, stacked along the (001) direction (growth direction), with 16 atoms in each layer. From these, we considered eight layers of Si atoms and four layers of Ge atoms, as can be seen in Fig. 1. For the heterostructure calculations, we used a Brillouin-zone sampling of four  $k$ -points corresponding to a (2 × 2 × 1) Monkhorst-Pack grid shifted by (1/2 1/2 1/2). In all calculations, the positions of all atoms in the supercell were allowed to relax until all the forces were smaller than 0.02 eV/Å. The unit-cell vectors perpendicular to the growth direction were kept fixed throughout

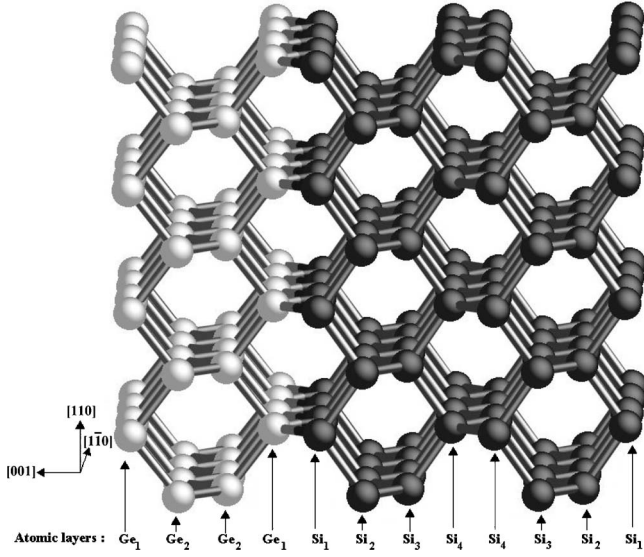


FIG. 1. Schematic view of the Si/Ge heterostructure composed of 12 atomic layers stacked along the (001) direction. There are eight layers of Si atoms and four layers of Ge atoms. The subscripts are used to label the inequivalent (by symmetry) layers.

the calculations, with a magnitude equal to the calculated silicon lattice constant of  $a_{\text{Si}} = 5.46 \text{ \AA}$ . This was done in order to simulate the silicon substrate. In this way, the Ge atomic layers are under a biaxial strain, which could be relieved in real heterostructures by intermediate  $\text{Si}_{1-x}\text{Ge}_x$  layers. However, this does not affect our conclusions since both the  $\text{Mn}_{\text{Ge}}$  and the  $\text{Mn}_{\text{Si}}$  formation energies do not vary significantly with the lattice parameter.<sup>5</sup> The length of the unit cell along the growth direction was always optimized through the minimization of the total energy. As a final technical note, for all impurity calculations, we have not fixed the value of the total spin of the supercell. In all calculations, we used as an initial guess a Mn high-spin configuration, and after electronic and ionic relaxations, the total spin of the system was always equal to  $S=3/2$ .

### III. RESULTS AND DISCUSSION

The Si/Ge heterostructure in our calculations was constructed in such a way that by symmetry there is a total of four inequivalent Si layers, which will be labeled as  $\text{Si}_{(i)}$  ( $i=1, 2, 3$ , and  $4$ ), and two inequivalent Ge layers, which will be labeled as  $\text{Ge}_{(i)}$  ( $i=1$  and  $2$ ), as can be seen in Fig. 1. The Mn impurity was placed at tetrahedral interstitial sites as well as at substitutional sites in each of these six layers. The formation energy of an interstitial neutral impurity  $E_f^I$  is calculated as

$$E_f^I = E_{\text{def}} - E_{\text{het}} - \mu_{\text{Mn}}, \quad (1)$$

where  $E_{\text{def}}$  is the total energy of the supercell with the Mn atom at the interstitial site,  $E_{\text{het}}$  is the total energy of the heterostructure without the Mn impurity, and  $\mu_{\text{Mn}}$  is the Mn chemical potential. For the substitutional Mn calculations, we replaced either a Si or a Ge atom by the Mn impurity. The formation energy  $E_f^S$  is given by

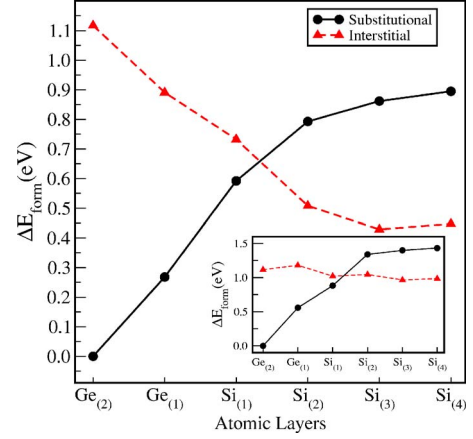


FIG. 2. (Color online) Formation energies of the Mn impurity at different substitutional (circles) and tetrahedral interstitial (triangles) sites in the Si/Ge heterostructure. The energies are relative to that of the impurity at the substitutional site in the  $\text{Ge}_2$  layer. The calculations were performed using a value for the Mn chemical potential  $\mu_{\text{Mn}}$  obtained by assuming  $\text{MnSi}$  as the source of Mn atoms. In the inset, we present the formation energies for the same structures, but using a Mn chemical potential that varies from layer to layer depending on its local neighborhood. See text for details. The lines are guides to the eye.

$$E_f^S = (E_{\text{def}} + \mu_X) - E_{\text{het}} - \mu_{\text{Mn}}, \quad (2)$$

where  $\mu_X$  is the chemical potential of either Si or Ge.

In Fig. 2, we present our results, obtained using Eqs. (1) and (2), for the Mn impurity at substitutional and interstitial sites in the inequivalent Si and Ge layers. As expected, in the Ge layer the substitutional Mn impurity has a lower formation energy than the interstitial Mn, whereas the opposite result is obtained for all Si layers except at the Si-Ge interface. In the most bulklike Ge layer,  $\text{Ge}_{(2)}$ , we obtained the difference in formation energies between the interstitial and substitutional sites to be  $\Delta E_{I-S} = 1.12 \text{ eV}$ . This should be contrasted to a formation energy difference of the bulk,  $\Delta E_{I-S} = 0.77 \text{ eV}$ .

This large increase can be attributed to the compressed Ge lattice parameter, which tends to increase the  $\text{Mn}_I$  formation energy.<sup>5</sup> At the most bulklike Si layer,  $\text{Si}_{(4)}$ , on the other hand, the difference between the substitutional and interstitial formation energies is  $\Delta E_{I-S} = -0.45 \text{ eV}$ , which is quite close to the value obtained for the bulk,  $\Delta E_{I-S} = -0.42 \text{ eV}$ . This is reasonable since the Si layers have the bulk lattice parameter. At the Si/Ge interface, we obtain  $\Delta E_{I-S} = 0.62 \text{ eV}$  at the  $\text{Ge}_{(1)}$  layer and  $\Delta E_{I-S} = 0.14 \text{ eV}$  at the  $\text{Si}_{(1)}$  layer. Even though this is nominally a Si layer, in this case the substitutional impurity has a lower formation energy than the interstitial. This is a consequence of Mn having two Si and two Ge as nearest neighbors. This kind of trend has already been observed for Mn in SiGe alloys,<sup>5</sup> where in Si-rich neighborhoods the interstitial is more stable than the substitutional impurity, whereas a reversal of this tendency occurs as the neighborhood becomes richer in Ge.

From these results, one can see that the overall lowest formation energy is that of  $\text{Mn}_{\text{Ge}}$  in the most bulklike Ge

layer, i.e.,  $\text{Ge}_{(2)}$ , which is 0.45 eV lower than the formation energy of an interstitial Mn at the  $\text{Si}_{(4)}$  layer. This indicates that the Mn impurities are thermodynamically stable in the Ge layers. Another important point is that for Mn impurities in the  $\text{Ge}_{(2)}$  layer, the lower bound for diffusion is 1.12 eV, which is given by the difference between the formation energies of an interstitial and a substitutional impurity in the  $\text{Ge}_{(2)}$  layer. This means that the impurity is kinetically stable in this layer because the migration barrier is much larger than the typical thermal energy. From these arguments, we expect that the Mn migration towards the Si substrate should be negligible. The calculations were performed using a value for the Mn chemical potential  $\mu_{\text{Mn}}$  obtained by assuming MnSi as the source of Mn atoms. Even though the magnitudes of the formation energies may change for other choices<sup>5</sup> of  $\mu_{\text{Mn}}$ , we observed that the main conclusions remain unaffected by the choice of chemical potential. In order to illustrate this point, we present in the inset of Fig. 2 the formation energies for the same structures, but using a Mn chemical potential that varies from layer to layer depending on its local neighborhood. We used the general expression for the Mn chemical potential in a  $\text{Si}_{1-x}\text{Ge}_x$  alloy,<sup>5</sup>  $\mu_{\text{Mn}}(x)$ , given by  $\mu_{\text{Mn}}(x) = (1-x)\mu_{\text{MnSi}} + x\mu_{\text{MnGe}} - \mu_{\text{Si}}(1-x) - \mu_{\text{Ge}}x$  (see Ref. 5 for details). In our case, we used  $1-x$  and  $x$  as the numbers of Si and Ge nearest neighbors of Mn, respectively. Therefore, for the  $\text{Ge}_{(2)}$  layer we have  $x=1$ , for the  $\text{Ge}_{(1)}$  and  $\text{Si}_{(1)}$  layers we have  $x=0.5$ , and for the other Si layers we have  $x=0$ . As can be seen in the inset, the main conclusion that the substitutional Mn in the Ge layers are more stable than the interstitial Mn in the Si layers remains valid, with even an increase in the formation energy differences. Regarding the choice of the Ge chemical potential for the calculation of the substitutional Mn impurity, its value is always very close to the  $\mu_{\text{Ge-bulk}}$ , whether one considers a Ge-poor or a Ge-rich condition, as explained in Ref. 5. Therefore, the choice of the Ge chemical potential does not change any conclusion, but it changes the numerical values by less than 0.01 eV. Finally, the Si chemical potential was always fixed at the  $\mu_{\text{Si-bulk}}$ . However, as for the  $\mu_{\text{Ge}}$ , changes in this choice would not alter the results.<sup>5</sup>

We have also investigated the character of the net local magnetization, defined as  $m(\mathbf{r}) = \rho_{\text{up}}(\mathbf{r}) - \rho_{\text{down}}(\mathbf{r})$ , for the Mn in its most stable configuration, viz., at a substitutional site in the Ge bulklike layer,  $\text{Ge}_{(2)}$ . The behavior of the net local magnetization is illustrated in Fig. 3. As can be seen, the net spin is highly localized around the Mn atom, with an anti-parallel spin-density contribution at its four Ge nearest neighbors, which is similar to what was observed for Mn in GaAs (Refs. 12 and 13) and in Ge bulk. The net integrated value of  $m(\mathbf{r})$  is  $3.00\mu_B$  for the supercell. We conclude that in the heterostructure, the magnetic moment has a behavior that is similar to what we found for pure Ge.

In order to study the character of the exchange interaction between Mn impurities in the Ge layers, we performed some calculations for two Mn atoms in the  $\text{Ge}_{(2)}$  layer. As a sampling of the possible couplings, we considered three Mn-Mn distances equal to 3.41, 5.40, and 7.73 Å. We obtained a Mn-Mn antiferromagnetic ground state in all cases.

Another important question is how this coupling depends on the substrate lattice constant, which depends on the Ge

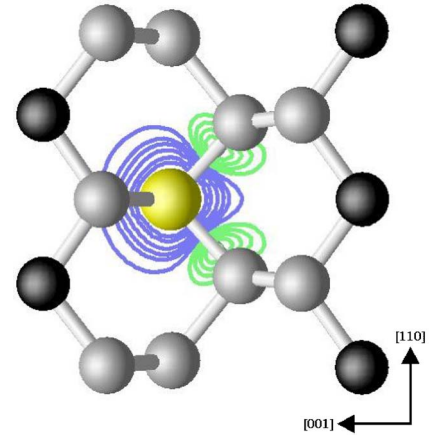


FIG. 3. (Color online) Contour plots (in  $e/\text{Å}^3$ ) of the local magnetization  $m(\mathbf{r}) = \rho_{\text{up}}(\mathbf{r}) - \rho_{\text{down}}(\mathbf{r})$  for the substitutional Mn in the  $\text{Ge}_{(2)}$  layer, in a plane that contains Mn (yellow sphere) and two of its Ge nearest neighbors. One can see that the Mn moment is rather localized. The darker (lighter) spheres denote Si (Ge) atoms. The outermost (innermost) green line has  $m(\mathbf{r}) = -0.01$  ( $m(\mathbf{r}) = -0.04$ ). The innermost (outermost) blue line has  $m(\mathbf{r}) = 0.4$  ( $m(\mathbf{r}) = 0.01$ ).

content  $x$  for a  $\text{Si}_x\text{Ge}_{1-x}$  alloy. In order to gain insight on this dependence, we performed calculations for four substrate lattice constants, corresponding to  $x=1, 0.75, 0.5$ , and  $0.25$ . Note that we always use the same structure that we have been using so far. We only change the lateral size of our supercell, assuming that the Vegard law is a good approximation for the  $\text{Si}_x\text{Ge}_{1-x}$  lattice parameter.<sup>14</sup> These calculations were performed for the Mn-Mn atoms as second-nearest neighbors in the  $\text{Ge}_{(2)}$  layer. In Table I, we observe that (i) as already mentioned, at the Si ( $x=1$ ) lattice constant, the Mn-Mn coupling is antiferromagnetic; (ii) as  $x$  increases, thus increasing the lattice constant, the Mn-Mn coupling becomes ferromagnetic; and (iii) as the germanium lattice is approached, the Mn-Mn coupling increases. For the Ge bulk ( $x=0$ ), we obtain a ferromagnetic interaction with  $\Delta E_{\text{AFM-FM}} = 110$  meV.

In Fig. 4, we plot the net local magnetization,  $m(\mathbf{r}) = \rho_{\text{up}}(\mathbf{r}) - \rho_{\text{down}}(\mathbf{r})$ , around the two Mn atoms. The two top panels [Figs. 4(a) and 4(b)] correspond to the substrate lattice constant equal to the Si one ( $x=1$  result of Table I), whereas the two lower panels [Figs. 4(c) and 4(d)] corre-

TABLE I. Total energy differences between an antiferromagnetic and ferromagnetic coupling,  $\Delta E_{\text{AFM-FM}}$ , between two Mn atoms positioned as second-nearest neighbors in the  $\text{Ge}_{(2)}$  layer. The calculations are for different substrate lattice constants chosen to mimic a  $\text{Si}_x\text{Ge}_{1-x}$  alloy. See text for details.

Substrate lattice constant	$\Delta E_{\text{AFM-FM}}$ (meV)	Mn-Mn distance (Å)
Si	-3.0	3.41
$\text{Si}_{0.75}\text{Ge}_{0.25}$	19.0	3.59
$\text{Si}_{0.50}\text{Ge}_{0.50}$	41.0	3.68
$\text{Si}_{0.25}\text{Ge}_{0.75}$	64.0	3.76

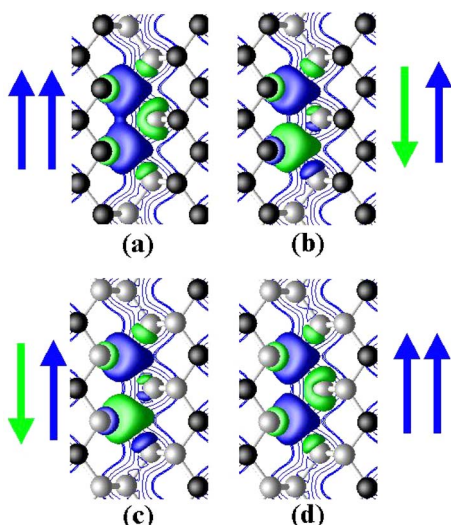


FIG. 4. (Color online) Isosurfaces for the net local magnetization  $m(\mathbf{r}) = \rho_{up}(\mathbf{r}) - \rho_{down}(\mathbf{r})$  in the case of two  $\text{Mn}_{\text{Ge}}$  in the  $\text{Ge}_{(2)}$  layer. The two top panels [(a) and (b)] correspond to the substrate lattice constant equal to the Si one ( $x=1$  result of Table I), whereas the two lower panels [(c) and (d)] correspond to the substrate lattice constant of a  $\text{Si}_{0.25}\text{Ge}_{0.75}$  alloy. The rightmost panels in both cases show the lowest-energy configurations. The blue (green) surfaces correspond to  $m(\mathbf{r}) = 0.015e/\text{\AA}^3$  ( $m(\mathbf{r}) = -0.015e/\text{\AA}^3$ ). The darker (lighter) spheres denote Si (Ge) atoms.

spond to the substrate lattice constant of a  $\text{Si}_{0.25}\text{Ge}_{0.75}$  alloy. The rightmost panels in both cases show the lowest-energy configurations. For the substrate with the Si lattice constant, the Mn-Mn coupling favors an antiparallel alignment between the Mn magnetic moments, whereas for the substrate with the  $\text{Si}_{0.25}\text{Ge}_{0.75}$  lattice parameter, a parallel alignment has the lowest energy. In the former case, the distance be-

tween the Mn atoms is equal to  $3.41 \text{\AA}$ , and it increases to  $3.76 \text{\AA}$  in the latter situation. The Pauli repulsion between the Mn  $d$ -electrons is probably the cause of the antiparallel alignment when the Mn atoms are too close for the substrate Si lattice constant. It is known that in  $\text{Ga}_{1-x}\text{Mn}_x\text{N}$  film surfaces,<sup>15</sup> the antiferromagnetic (AFM) state is mediated by bond-length contraction. In our study, the bond-length contraction in the Si/Ge interface would be caused by the substrate lattice constant, playing an important role in the Mn-Mn coupling.

#### IV. CONCLUSION

In summary, we have performed a systematic study, using total-energy *ab initio* calculations, of the relative stability of substitutional and interstitial Mn impurities in Si/Ge heterostructures. We have obtained the significant result that  $\text{Mn}_{\text{Ge}}$  at bulklike Ge layers are the most stable configurations of the impurity. Moreover, there is a large diffusional barrier that also makes the Mn in Ge kinetically stable. This means that if one grows  $\text{Mn}_x\text{Ge}_{1-x}$  layers on top of Si substrates, Mn will not tend to migrate towards the Si substrate. The Mn-Mn interactions, in the most bulklike Ge layer, lead to an antiferromagnetic ground state for a substrate with the Si lattice constant. However, increasing this lattice constant with the use of a  $\text{Si}_{1-x}\text{Ge}_x$  substrate changes the Mn-Mn interaction to a ferromagnetic one, which may allow these systems to be used in type-IV semiconductor spintronic devices.

#### ACKNOWLEDGMENTS

We acknowledge the support from the Brazilian agencies FAPESP and CNPq. One of us (A.A.) acknowledges the support from FAEP-UNICAMP.

<sup>1</sup> See Refs. 2 and 3 for comprehensive reviews on the properties of DMS materials.

<sup>2</sup> I. Žutić, J. Fabian, and S. Das Sarma, *Rev. Mod. Phys.* **76**, 323 (2004).

<sup>3</sup> A. H. MacDonald, P. Schiffer, and N. Samarth, *Nat. Mater.* **3**, 195 (2005).

<sup>4</sup> Y. D. Park, A. Wilson, A. T. Hanbicki, J. E. Mattson, T. Ambrose, G. Spanos, and B. T. Jonker, *Appl. Phys. Lett.* **78**, 2739 (2001).

<sup>5</sup> Antônio J. R. da Silva, A. Fazzio, and A. Antonelli, *Phys. Rev. B* **70**, 193205 (2004).

<sup>6</sup> H. H. Woodbury and G. W. Ludwig, *Phys. Rev.* **117**, 102 (1960).

<sup>7</sup> H. Nakashima and K. Hashimoto, *J. Appl. Phys.* **69**, 1440 (1991).

<sup>8</sup> Y. Kamon, H. Harima, A. Yanase, and H. Katayama-Yoshida,

*Physica B* **308-310**, 391 (2001).

<sup>9</sup> J. P. Perdew and Y. Wang, *Phys. Rev. B* **45**, 13244 (1992).

<sup>10</sup> D. Vanderbilt, *Phys. Rev. B* **41**, 7892 (1990).

<sup>11</sup> G. Kresse and J. Hafner, *Phys. Rev. B* **47**, 558 (1993); G. Kresse and J. Furthmüller, *ibid.* **54**, 11169 (1996).

<sup>12</sup> A. J. R. da Silva, A. Fazzio, R. R. dos Santos, and L. E. Oliveira, *Physica B* **340-342**, 874 (2003).

<sup>13</sup> A. J. R. da Silva, A. Fazzio, R. R. dos Santos, and L. E. Oliveira, *J. Phys.: Condens. Matter* **16**, 8243 (2004).

<sup>14</sup> P. Venezuela, G. M. Dalpian, Antônio J. R. da Silva, and A. Fazzio, *Phys. Rev. B* **64**, 193202 (2001).

<sup>15</sup> Q. Wang, Q. Sun, P. Jena, and Y. Kawazoe, *Phys. Rev. Lett.* **93**, 155501 (2004).